*MAT_PAPER and *MAT_COHESIVE_PAPER:
Two New Models for Paperboard Materials

Jesper Karlsson[1], Mikael Schill[1], Johan Tryding[2]
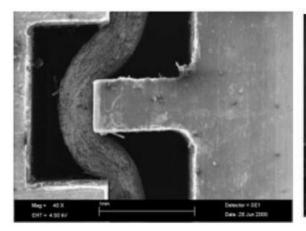
[1]*DYNAmore Nordic, Sweden,* [2]*Tetra Pak, Sweden*

Abstract

*We here present two new material models for the modeling of paperboard materials. The main motivation for the models is to accurately simulate the production of food and beverage containers for the packaging industry. The main material, ***MAT_PAPER**, is an orthotropic elastoplastic model that supports both solid and shell elements. In conjunction, an elastoplastic cohesive material, ***MAT_COHESIVE_PAPER**, is introduced to simulate delamination. Simulations of bending and creasing of paperboard using these new materials, performed in collaboration with Tetra Pak, has shown good correlation with experimental results*

Introduction

Paperboard is a widely used material for packaging of food and beverages. To ensure the quality of the contents the container needs to be aseptic, e.g. the paperboard may not contain cracks that could jeopardize the structural integrity. Such cracks could form during the manufacturing and filling of the container.

Forming paperboard into a container is a two stage process. The paperboard has to be folded, and to accommodate for the folding, the process is preceded by a creasing process stage. The purpose of the creasing stage is to notch the paperboard and weaken the fiber structure, see Fig. 1. This will enable further delamination and a predetermined direction for the fold.
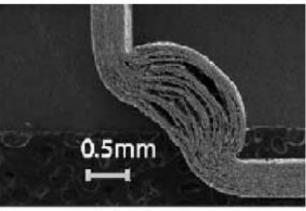

Fig. 1: Creasing of paperboard (left), from Dunn [1] and folding (right) from Nagasawa et al. [2].

Paperboard properties

Paperboard consists mainly of cellulose fibers. Due to its fibrous structure, the directions and bonding of the fibers will have a major influence on the paperboard properties. Due to the

manufacturing process an orthotropic material is typically produced where the properties are defined in machine (MD), cross (CD) and thickness (ZD) directions, see Fig. 2.
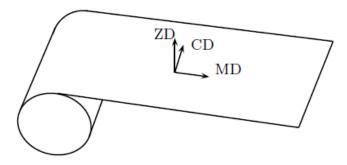

Fig. 2: Illustration of the paperboard orthotropic directions, from Borgqvist [3].

The paperboard can consist of a single ply or multiple plies of different thickness and properties. Also, the paperboard can be joined with layers of aluminum foil and/or polyethylene as liquid and light barriers. More details on material testing of paperboard and paperboard properties can be found in e.g. Tryding [4], Mäkelä et al. [5] and Nygårds [6].

In-plane properties

The in-plane properties are typically identified through simple tensile tests in MD, CD and 45 degree directions. Tests are performed for each ply if applicable, see Fig. 3, and typically show a highly anisotropic material, as expected. Also, there is a big difference between the different plies. From Fig. 3 it is clear that the deformation consists of an elastic and a plastic region.
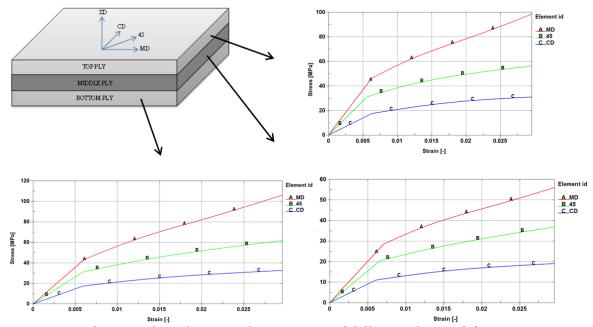

Fig. 3: Typical in-plane tensile properties of different plies and directions.

The properties in compression are determined by using a custom made testing equipment that uses static compression in ZD to avoid out-of-plane buckling. The properties are linear up to the maximum point where it is assumed that out-of-plane effects are dominant, see Fig. 4.
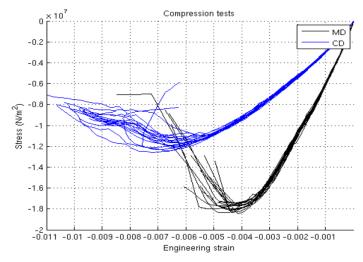

Fig. 4: Typical in-plane compressive properties, from Lindström [7].

Out-of-plane properties

In out-of-plane tension, paperboard shows a linear behavior up to the point of delamination, see Fig. 5(a). In out-of-plane compression, the material is non-linear elastic-plastic, see Fig. 5(b).
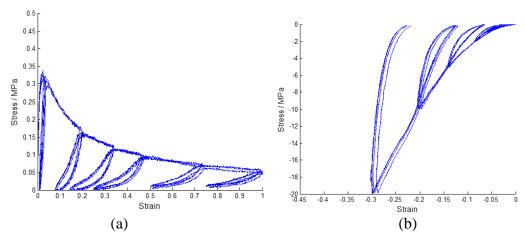

(a)   (b)

Fig. 5: Typcial out-of-plane tension (a) and compression (b).

In out-of-plane shear, the material shows a dependency on the ZD compressive stress, where the shear strength increases with increasing ZD stress, see Fig. 6.
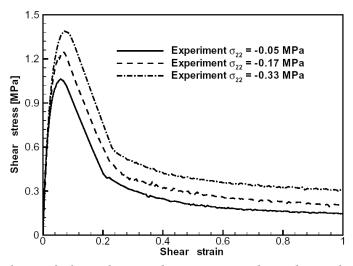
Fig. 6: Typical out-of-plane shear and its ZD stress dependency, from Stenberg [8].

From Fig. 5 and Fig. 6 it is evident that the out of plane tension and shear behavior shows a softening behavior. This is due to delamination of the paperboard. To accommodate for this, a cohesive model will be used.

*MAT_PAPER

A paper material model based on Xia [8] and Nygårds et al. [9] was implemented in LS-DYNA$^{®}$ and is available from R8. The material model is denoted *MAT_PAPER and is material type 274. It has a solid element version which is hyperelastic-plastic, and a shell element version which is hypoelastic-plastic. In the following, the solid element version is described. The implementation is based on an assumption that the in-plane and out-of plane models are uncoupled and thus solved separately.

The stress-strain relationship for solid elements is based on a multiplicative split of the deformation gradient into an elastic and a plastic part

$$\mathbf{F} = \mathbf{F}_e \mathbf{F}_p,$$

where the plastic deformation gradient is given by the evolution

$$\dot{\mathbf{F}}_p = \mathbf{L}_p \mathbf{F}_p,$$

for the plastic velocity gradient

$$\mathbf{L}_p = \begin{bmatrix} \dot{\varepsilon}_p^f \dfrac{\partial f}{\partial S_{11}} & \dot{\varepsilon}_p^f \dfrac{\partial f}{\partial S_{12}} & \dot{\varepsilon}_p^h \dfrac{\partial h}{\partial S_{13}} \\[2ex] \dot{\varepsilon}_p^f \dfrac{\partial f}{\partial S_{12}} & \dot{\varepsilon}_p^f \dfrac{\partial f}{\partial S_{22}} & \dot{\varepsilon}_p^h \dfrac{\partial h}{\partial S_{23}} \\[2ex] \dot{\varepsilon}_p^h \dfrac{\partial h}{\partial S_{13}} & \dot{\varepsilon}_p^h \dfrac{\partial h}{\partial S_{23}} & \dot{\varepsilon}_p^g \dfrac{\partial g}{\partial S_{33}} \end{bmatrix},$$

where f, g and h corresponds to the in-plane, out-of-plane and transverse shear yield surfaces, respectively.

The elasticity is modeled as orthotropic where the 2nd Piola-Kirchoff stress is given as

$$\mathbf{S} = \mathbf{C}\mathbf{E}_e,$$

where $\mathbf{C}$ is the typical constitutive matrix for an linear elastic orthotropic material and the elastic Green strain is formed as

$$\mathbf{E}_e = \frac{1}{2}(\mathbf{F}_e^{\mathrm{T}}\mathbf{F}_e - \mathbf{I}).$$

In-plane plasticity

The in-plane yield surface is constructed by six different yield planes:

1. Tension in MD

2. Tension in CD

3. Positive in-plane shear

4. Compression in MD

5. Compression in CD

6. Negative in-plane shear.

The yield planes are combined to an in-plane yield surface using

$$f = \sum_{i=1}^{6}\left[\frac{S:N_i}{q_i(\varepsilon_p^f)}\right]^{2k} - 1 \le 0$$

where N_i is the normal direction to the respective yield planes, k is a positive integer, q_i is the respective hardening function and ε_p^f is the in-plane plastic strain, see the LS-DYNA Keyword User's Manual [11] for details. A typical yield surface is shown in Fig. 7.
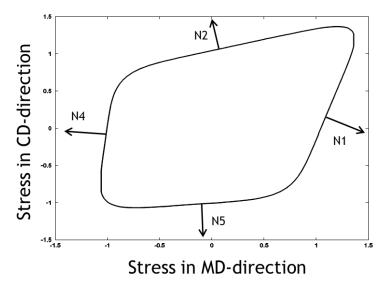

Fig. 7: In-plane yield surface.

Out-of-plane elasticity and plasticity

In out-of-plane compression, the stress is modified as

$$S_{33} = C_{31}E_{11}^e + C_{32}E_{22}^e + E_3^c\left[1 - e^{-C_cE_{33}^e}\right],$$

to model a non-linear elastic compressive behavior using material constants E_3^c and C_c. In out-of-plane tension, the material model is always elastic since the cohesive model described below will describe the delamination. However, in out-of-plane compression, the yield surface is given as

$$g = \frac{-S_{33}}{A_\sigma + B_\sigma e^{-C_\sigma \varepsilon_p^g}} - 1 \le 0,$$

where A_σ, B_σ and C_σ are hardening constants and ε_p^g is the out-of-plane compression plastic strain. The transverse shear yield surface is given as

$$h = \frac{\sqrt{S_{13}^2 + S_{23}^2}}{\tau_0 + [A_\tau - S_{33}B_\tau]\varepsilon_p^h} - 1 \le 0,$$

where τ_0, A_τ and B_τ are hardening parameters where the latter controls the influence from the out-of-plane compression stress. The transverse shear plastic strain is denoted ε_p^h.

*MAT_COHESIVE_PAPER

To model delamination, an elasto-plastic cohesive model was implemented in LS-DYNA for use in conjunction with *MAT_PAPER, and will be available in R9. The material model is denoted *MAT_COHESIVE_PAPER and is material type 279. As in *MAT_PAPER, the in-plane and out-of-plane models are uncoupled, but can be related through input data, i.e. by defining the in-plane traction parameters as curves of the normal traction.

Cohesive materials typically relate absolute separation δ to traction T through a cohesive law. The separation (related to distance between the cohesive element nodes) and traction are split up into a normal and a tangential contribution, where the latter is corresponding to out-of-plane shear.
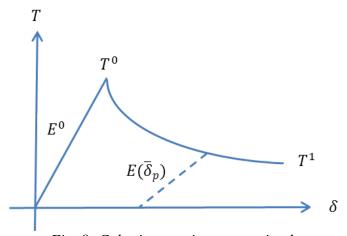

Fig. 8: Cohesive traction-separation law.

In Fig. 8, the cohesive law for the tangential traction and normal tensile traction is depicted, see Fig. 5 and Fig. 6 for comparison with typical experimental behavior. It is linearly elastic up to the peak traction T_0 after which the material is irreversibly damaged and starts to yield, with final yield traction T_1. Unloading is elastic with stiffness depending on maximum separation. Note that the option of a non-zero yield traction T_1 is motivated to mimic friction between the layers in the tangential direction.

The elasto-plastic model in normal compression is similar to *MAT_PAPER.

Normal tension
The total separation is modelled as an additive split of the elastic and plastic separation

$$\delta = \delta_e + \delta_p.$$

In normal tension ($\delta_e > 0$) the elastic traction is given by

$$T = E\delta_e = E(\delta - \delta_p) \geq 0,$$

where the tensile normal stiffness

$$E = (E_N^0 - E_N^1)\exp\left(\frac{-\bar{\delta}_p}{\delta_N}\right) + E_N^1,$$

depends on the effective plastic separation in the normal direction

$$\bar{\delta}_p = \int |\mathrm{d}\delta_p|.$$

Yield traction for tensile loads in normal direction is given by

$$T_{yield} = (T_N^0 - T_N^1)\exp\left(\frac{-\bar{\delta}_p}{\delta_N}\right) + T_N^1 \geq 0,$$

and yielding occurs when $T > T_{yield} \geq 0$.

The above elastoplastic model gives the traction-separation law depicted in Fig. 8.

Normal compression
In normal compression the elastic traction is

$$T = E_3^c(1 - \exp(-C_c\delta_e)) \leq 0,$$

and the yield traction is

$$T_{yield} = -\left(A_\sigma + B_\sigma \exp\left(-C_\sigma\bar{\delta}_p\right)\right) \leq 0,$$

with yielding if $T < T_{yield} \leq 0$. This is similar to the elasto-plastic model for out-of-plane compression in *MAT_PAPER.

Tangential traction

Assume the total separation is an additive split of the elastic and plastic separation in each in-plane direction

$$\delta_i = \delta_e^i + \delta_p^i, \qquad i = 1,2.$$

The elastic traction is given by

$$T_i = E\delta_e^i = E(\delta_i - \delta_p^i),$$

where the tensile normal stiffness

$$E = (E_T^0 - E_T^1) \exp\left(\frac{-\bar{\delta}_p}{\delta_T}\right) + E_T^1,$$

depends on the effective plastic separation

$$\bar{\delta}_p = \int d\delta_p, \qquad d\delta_p = \sqrt{\left(d\delta_p^1\right)^2 + \left(d\delta_p^2\right)^2}.$$

Yield traction is given by

$$T_{yield} = (T_T^0 - T_T^1) \exp\left(\frac{-\bar{\delta}_p}{\delta_T}\right) + T_T^1,$$

and yielding occurs when

$$T_1^2 + T_2^2 - T_{yield}^2 \geq 0.$$

The plastic flow increment follows the flow rule

$$d\delta_p^i = \frac{T_i}{\sqrt{T_1^2 + T_2^2}} d\delta_p.$$

The above elastoplastic model gives the traction-separation law depicted in Fig. 8..

A creasing example

In this example a large scale creasing roller simulation is demonstrated. For more simulations and validation with experimental data, see Schill et. al. [12].

The paperboard consists of eight layers of shell elements (ELFORM=16) using *MAT_PAPER, and seven layers of cohesive elements (ELFORM=20) using *MAT_PAPER_COHESIVE. The layers build up three plies of paperboard, i.e. the cohesive shells are not only between plies but also located within a ply. Material data are taken from Tryding et. al. [10] and approximately 1.7 million shell elements and 1.3 million solid elements are used. See Fig. 9 for the setup.
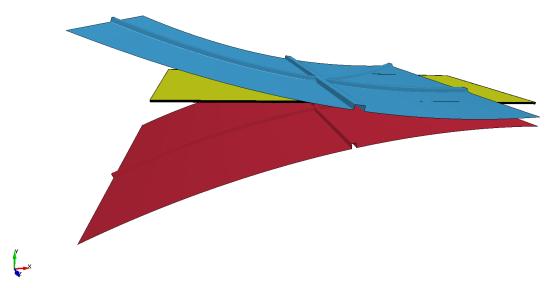
Fig. 9. Creasing of paper between rolls. Initial configuration.

During the creasing process several unwanted "wild" creases occur far away from the creasing lines. This is a result of compressive forces in the in-plane direction causing the paperboard to buckle and fold over itself, see Fig. 10. It is a well-known and unwanted phenomenon that may cause a loss of the aseptic properties of the packaging. In Fig. 11 a close up the wild crease can be seen. It is clear that layers have started to delaminate and due to the large separations some elements erode. Maximum separation is set as a material parameter in the cohesive material.

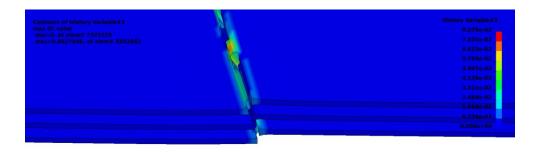*Fig. 10. Final creases and wild creases (see e.g. bottom edge).*

Fig. 11. Close up of wild crease at bottom edge. Every other cohesive element is shown together with effective plastic strain in the normal direction.

Summary

Two new models for modelling of paperboard now exists in LS-DYNA: *MAT_PAPER and *MAT_COHESIVE_PAPER. These models are to be used together to properly simulate delamination in paper materials. In Schill et. al. [12], *MAT_PAPER was presented and evaluated in detail. In this paper, *MAT_COHESIVE_PAPER is presented and used in a large scale simulation.

References

[1] Dunn, H.: "Micromechanics of paperboard deformation", Master's thesis, Massachusetts Institute of Technology, 2000

[2] Nagasawa, S., Endo, R., Fukuzawa, Y.,Uchino, S. and Katayama, I.: "Creasing characteristic of aluminium coated paperboard", Journal of Materials Processing Technology, 201(1-3), 2000 , 401-407

[3] Borgqvist, E.: "Continuum modeling of the mechanical properties of paperboard", Licentiate Dissertation, Lund University, 2014

[4] Tryding, J.: "In plane fracture of paper", PhD Thesis, Lund Institute of Technology, 1996

[5] Mäkelä, P., Östlund, S.:"Orthotropic elastic-plastic material model for paper materials", International Journal of Solids and Structures, 40 (21), 2003, 5599-5620

[6] Nygårds, M.: "Experimental techniques for characterization of elastic-plastic material properties in paperboard", Nordic Pulp and Paper Research Journal, 23 (4), 2008, 432-437

[7] Lindström, T.: "In-plane paperboard model", Master's Thesis, Lund Institute of Technology, 2013

[8] Stenberg, N.: "On the Out-of-Plane Mechanical Behaviour of Paper Materials", PhD Thesis, Royal Institute of Technology, Stockholm, 2002

[9] Xia, Q. S.: "Mechanics of inelastic deformation and delamination in paperboard", PhD Thesis, Massachusetts Institute of Technology, 2002

[10]   Nygårds, M., Just, M. and Tryding, J.: "Experimental and numerical studies of creasing of paperboard", International Journal of Solids and Structures, 46, 2009, 2493-2505

[11]   LS-DYNA Keyword User's Manual, R8.0, Volume I-II, Livermore Technology Software Corporation (LSTC), March 2015.

[12]   Schill, M., Tryding, J., Karlsson:"Simulation of forming of paperboard packaging using LS-DYNA", 10th European LS-DYNA Conference 2015, Würtzburg, Germany.